

1 **Trends and spatial shifts in lightning fires and smoke concentrations**  
2 **in response to 21<sup>st</sup> century climate over the national forests and parks**  
3 **of the western United States**

4 Yang Li<sup>1</sup>, Loretta J. Mickley<sup>1</sup>, Pengfei Liu<sup>1</sup>, and Jed O. Kaplan<sup>2</sup>

5 <sup>1</sup>John A. Paulson School of Engineering and Applied Sciences, Harvard University, Cambridge,  
6 MA, USA

7 <sup>2</sup>Department of Earth Sciences, The University of Hong Kong, Hong Kong, China

8 *Correspondence to:* Yang Li ([yangli@seas.harvard.edu](mailto:yangli@seas.harvard.edu))

9

10 **Abstract.** Almost US\$ 3bn per year is appropriated for wildfire management on public land in the  
11 United States. Recent studies have suggested that ongoing climate change will lead to warmer and  
12 drier conditions in the western United States with a consequent increase in the number and size of  
13 wildfires, yet large uncertainty exists in these projections. To assess the influence of future changes  
14 in climate and land cover on lightning-caused wildfires in the national forests and parks of the  
15 western United States and the consequences of these fires on air quality, we link a dynamic  
16 vegetation model that includes a process-based representation of fire (LPJ-LMfire) to a global  
17 chemical transport model (GEOS-Chem). Under a scenario of moderate future climate change  
18 (RCP4.5), increasing lightning-caused wildfire enhances the burden of smoke fine particulate  
19 matter (PM), with mass concentration increases of ~53% by the late-21<sup>st</sup> century during the fire  
20 season in the national forests and parks of the western United States. In a high-emissions scenario  
21 (RCP8.5), smoke PM concentrations double by 2100. RCP8.5 also shows enhanced lightning-  
22 caused fire activity, especially over forests in the northern states.

## 23 **1 Introduction**

24 Both the incidence and duration of large wildfires in the forests of the western United States  
25 have increased since the mid-1980s (Westerling et al., 2006; Abatzoglou and Williams, 2016),  
26 affecting surface levels of particulate matter (Val Martin et al., 2006; Val Martin et al., 2015), with  
27 consequences for human health (Liu et al., 2017) and visibility (Spracklen et al., 2009; Ford et al.,  
28 2018). Wildfire activity is influenced by a combination of different factors, including fuel load,  
29 fire suppression practices, land use, land cover change, and meteorology (Pechony and Shindell,  
30 2010). Over the forests of the western United States (WUS), lightning-caused wildfires account  
31 for the majority of burned area (Abatzoglou et al., 2016; Brey et al., 2018) and have driven most  
32 of the recent increase in large wildfires, with human ignition contributing less than 12% to this  
33 trend (Westerling, 2016). Studies suggest that a warming climate could enhance wildfires in the  
34 WUS (Yue et al., 2013; Abatzoglou and Williams, 2016), but quantifying future wildfire activity  
35 is challenging, given uncertainties in land cover trends and in the relationships between fire and  
36 weather. Not all these studies that attempt to predict future fire activity have accounted for  
37 changing land cover or have distinguished the effects of lightning fire ignitions from human-started  
38 fires. In this study, we project lightning-caused fire emissions and wildfire-specific PM  
39 concentrations over the national forests and parks of the WUS in the mid- and late- 21<sup>st</sup> century,  
40 using a dynamic global vegetation model combined with a chemical transport model. Our goal is  
41 to understand how trends in both land cover and meteorology may affect natural fire activity and  
42 smoke air quality over the 21<sup>st</sup> century.

43 Consistent with projections of increasing wildfire in the WUS, recent studies have also  
44 predicted enhancement of fire-generated PM (smoke PM; BC+OC) under a warmer and drier  
45 climate in this region (Yue et al., 2013; Yue et al., 2014; Spracklen et al., 2009; Ford et al., 2018;

46 Westerling et al., 2006). Some of these studies relied on statistical models that relate  
47 meteorological variables to fire metrics such as area burned; these models can then be applied to  
48 projections from climate models (Yue et al., 2013; Yue et al., 2014; Spracklen et al., 2009;  
49 Archibald et al., 2009; Wotton et al., 2003; Westerling and Bryant, 2008). However, these  
50 statistical methods do not account for changes in vegetation due to climate, increasing atmospheric  
51 CO<sub>2</sub> concentrations, or land use. A further weakness of these studies is that they do not consider  
52 whether enhanced fire activity in the future atmosphere may ultimately deplete the supply of  
53 woody fuels (Yue et al., 2013; Yue et al., 2014). Other studies have coupled global vegetation  
54 models to climate models to better represent such fire-vegetation-climate interactions (Chaste et  
55 al., 2018; Ford et al., 2018). Dynamic vegetation models with interactive fire modeling provide  
56 important estimates for long-term and large-scale changes in fire emissions, with most of these  
57 models simulating present-day fire emissions within the range of satellite products but failing to  
58 reproduce the interannual variability (Li et al., 2019; Hamilton et al., 2018). The coupled modeling  
59 approaches integrate vegetation dynamics, land-atmosphere exchanges, and other key physical  
60 processes, allowing consideration of many factors driving fire activity and smoke pollution on  
61 regional scales. Building on this research, we use an integrated vegetation-climate model system  
62 with the aim of clarifying how changing meteorology and vegetation together drive future  
63 lightning-caused wildfire activity. We also provide predictions of smoke pollution at finer spatial  
64 resolution than previously. Our approach accounts for the impact of future climate and lightning  
65 fires on fuel structure, and these fine-scale predictions are of greater utility to environmental  
66 managers and especially the health impacts community.

67         Lightning is the predominant cause of wildfire ignition in most mountainous and forest  
68 regions of the WUS during months that have high fire frequency (Abatzoglou et al., 2016; Balch

69 et al., 2017). In remote and mountainous terrain, anthropogenic ignitions are infrequent and >90%  
70 of total area burned is caused by lightning-started fires (Abatzoglou et al., 2016). Here we study  
71 lightning-caused fires over the national forests and parks of the WUS in the mid- and late- 21<sup>st</sup>  
72 century under two future climate change scenarios defined by Representative Concentration  
73 Pathways (RCPs). RCP4.5 represents a moderate pathway with gradual reduction in greenhouse  
74 gas (GHG) emissions after 2050, while RCP8.5 assumes continued increases in GHGs throughout  
75 the 21<sup>st</sup> century. We use the Lund-Potsdam-Jena-Lausanne-Mainz (LPJ-LMfire) Dynamic Global  
76 Vegetation Model (Pfeiffer et al., 2013) to simulate dynamic fire-vegetation interactions under  
77 future climate. LPJ-LMfire, which has been used previously to investigate historical fire activity  
78 (e.g., Chaste et al., 2018), is applied here to estimate natural fire emissions under future climate  
79 simulated by the Goddard Institute for Space Studies (GISS) Model E climate model. July, August,  
80 and September (JAS) are the months of greatest fire activity in WUS forests (Park et al., 2003) and  
81 the focus of our study. We limit the spatial extent of our analyses to the national forests and parks  
82 of the WUS, here defined as 31°N – 49°N, 100°W – 125°W.

83

## 84 **2 Methods**

85 We quantify the effects of changing climate on area burned and fire emissions caused by  
86 lightning over the national forests and parks in the WUS using the LPJ-LMfire model (Pfeiffer et  
87 al., 2013), driven by meteorological fields from the GISS-E2-R climate model (Nazarenko et al.,  
88 2015). Combined with emission factors from Akagi et al., 2011, dry matter burned calculated by  
89 LPJ-LMfire can be used to estimate natural wildfire emissions of black carbon (BC) and organic  
90 carbon (OC) particles, which are then passed to GEOS-Chem, a 3-D chemical transport model, to  
91 simulate the transport and distribution of wildfire smoke across the WUS. A flowchart of modeling

92 setup is included in the Supplement (Fig. S1).

## 93 **2.1 LPJ-LMfire**

94 The LPJ-LMfire dynamic vegetation model is driven by gridded climate, soil, land use  
95 fields, and atmospheric CO<sub>2</sub> concentrations, and simulates vegetation structure, biogeochemical  
96 cycling, and wildfire (Pfeiffer et al., 2013; Sitch et al., 2003). Wildfires are simulated based on  
97 processes including explicit calculation of lightning ignitions, the representation of multi-day  
98 burning and coalescence of fires, and the calculation of rates of spread in different vegetation types  
99 (Pfeiffer et al., 2013). LPJ-LMfire calculates fire starts as a function of lightning ground strikes  
100 and ignition efficiency. Not every lightning strike causes fire. The model accounts for the  
101 flammability of different plant types, fuel moisture, the spatial autocorrelation of lightning strikes,  
102 and previously burned area. As fires grow in size, the likelihood of fire coalescence or merging  
103 increases. Fires are extinguished by consuming the available fuel or by experiencing sustained  
104 precipitation (Pfeiffer et al., 2013). Our study does not consider changes in human-caused fires,  
105 including agricultural fires.

106 The climate anomaly fields from the GISS-E2-R climate model used to prepare a future  
107 scenario for LPJ-LMfire are monthly mean surface temperature, diurnal temperature range (i.e.,  
108 the difference between monthly mean daily maximum and daily minimum temperatures), total  
109 monthly precipitation, number of days in the month with precipitation greater than 0.1 mm,  
110 monthly mean total cloud cover fraction, and monthly mean surface wind speed. This version of  
111 the GISS model was configured for Phase 5 of the Coupled Model Intercomparison Project  
112 (CMIP5) (Nazarenko et al., 2015). For RCP4.5, the GISS model predicts a statistically significant  
113 increase in surface temperature of 1.4 K averaged over the entire region by 2050 during JAS; for  
114 RCP8.5, the mean JAS temperature increase is 3.7 K by 2100. In both future climate scenarios,

115 significant precipitation decreases of ~20% by 2100 are simulated. Several studies have predicted  
116 future increases in lightning due to climate change (e.g., Price and Rind, 1994a, Romps et al.,  
117 2014). However, the relationship between lightning flash rate and meteorology is poorly  
118 constrained in models and depends largely on physical parameters such as cold cloud thickness,  
119 cloud top height, or convective available potential energy. In our study, lightning strike density for  
120 application in LPJ-LMfire is calculated using the GISS convective mass flux following the  
121 empirical parameterization of Magi, 2015. Although observations suggest a link between aerosol  
122 load and lightning frequency (e.g., Altaratz et al., 2017), we do not consider that relationship here.  
123 Unlike surface temperature and precipitation, we find that average lightning density over the West  
124 does not change significantly during the 21<sup>st</sup> century, as described in Fig. S2. LPJ-LMfire scales  
125 lightning flashes to cloud-to-ground lightning strikes, which are the portion of total flashes in  
126 clouds that directly causes natural wildfires (Pfeiffer et al., 2013). Therefore, cloud-to-ground  
127 lightning frequencies are also considered constant during the 21<sup>st</sup> century. We run LPJ-LMfire on  
128 a 0.5°×0.5° global grid, though for this study only results over the national forests and parks of  
129 the WUS are analyzed.

130         The GISS-E2-R meteorology used here covers the period 1701-2100 at a resolution of 2°  
131 latitude x 2.5° longitude. The start year of the two climate scenarios, RCP4.5 and RCP8.5, is 2006.  
132 The two RCPs capture a range of possible climate trajectories over the 21<sup>st</sup> century, with radiative  
133 forcings at 2100 relative to pre-industrial values of +4.5 W m<sup>-2</sup> for RCP4.5 and +8.5 W m<sup>-2</sup> for  
134 RCP8.5. From 2011 to 2015, the greenhouse gas concentrations of the two scenarios are nearly  
135 identical. To downscale the GISS meteorological fields to finer resolution for LPJ-LMfire, we first  
136 calculate the 2010-2100 monthly anomalies relative to the average over the 1961-1990 period, and  
137 then add the resulting timeseries to a high-resolution observationally based climatology at 0.5°

138 latitude  $\times$  0.5° longitude spatial resolution. The climatology was prepared using the datasets  
139 including WorldClim 2.1, Climate WNA, CRU CL 2.0, Wisconsin HIRS Cloud Climatology, and  
140 LIS/OTD, as described in Pfeiffer et al., 2013. For each RCP, LPJ-LMfire simulates vegetation  
141 dynamics and fire continuously for the period 1701-2100, with monthly resolution. Continuous  
142 400-year simulations allow for sufficient spin-up. The LPJ-LMfire simulations used here cover the  
143 period 2006-2100. We apply future land use scenarios following the two RCPs in CMIP5, in which  
144 the extent of crop and pasture cover in the WUS increases by 30% in future climates, with most of  
145 these changes occurring outside the national forest and park lands in the region (Brovkin et al.,  
146 2013; Kumar et al., 2013).

147       Passive fire suppression results from landscape fragmentation caused by land use (e.g., for  
148 crop and grazing land, roads, and urban areas), and this influence on fire activity is included in the  
149 LPJ-LMfire simulations (Pfeiffer et al., 2013). The model does not, however, consider the active  
150 fire suppression practiced throughout much of the WUS. We therefore limit our study to wildfire  
151 activity on the national forest and park lands of the WUS that are dominated by lightning fires and  
152 where land use for agriculture and urban areas is minimal. To focus only on national forest and  
153 park lands, we apply a 0.5°  $\times$  0.5° raster across the WUS that identifies the fraction of each grid  
154 cell that belongs to a national forest or national park (Fig. S3), and we consider only these areas in  
155 our analysis. To calculate fire emissions, we multiply the simulated dry matter burned by the  
156 fraction of national forest or park within each grid cell.

## 157 **2.2 Fire emissions**

158       Fuel biomass in LPJ-LMfire is discretized by plant functional type (PFT) into specific live  
159 biomass and litter categories, and across four size classes for dead fuels. The model simulates  
160 monthly values of total dry matter burned for nine PFTs as in Pfeiffer et al., 2013. To pass LPJ-

161 LMfire biomass burning emissions to GEOS-Chem, we first reclassify these nine PFTs into the  
162 six land cover types considered by GEOS-Chem. See Table S1 for a summary of the  
163 reclassification scheme. Tropical broadleaf evergreen, tropical broadleaf raingreen, and C<sub>4</sub> grasses  
164 are not simulated by LPJ-LMfire in the national forests and parks of the WUS. Emission factors  
165 based on the six land cover types in GEOS-Chem are then applied to dry matter burned from  
166 LPJ-LMfire, resulting in monthly BC and OC emissions over national forests and parks. These  
167 factors are from Akagi et al., 2011. As lightning-started wildfires are dominant over the WUS  
168 forests, an evaluation of fire emissions over national forest and park lands from the LPJ-LMfire  
169 model against the Global Fire Emissions Database (GFED4s) inventory (Giglio et al., 2013) is  
170 included in the Supplement (Fig. S4).

### 171 **2.3 GEOS-Chem**

172 We use the GEOS-Chem chemical transport model (version 12.0.1;  
173 <http://acmg.seas.harvard.edu/geos/>). We first carry out a global simulation at 4° latitude x 5°  
174 longitude spatial resolution, and then downscale to 0.5° × 0.625° over the WUS via grid nesting  
175 over the North America domain. For computational efficiency, we use the aerosol-only version of  
176 GEOS-Chem, with monthly mean oxidants archived from a full-chemistry simulation, as described  
177 in Park et al., 2004. Simulations with the fine-scale GEOS-Chem are computationally expensive,  
178 and we first test whether performing five-year simulations will adequately capture the interannual  
179 variability in fire activity generated by the LPJ-LMfire model. We take the average of fire-season  
180 total dry matter burned over five-year time slices in different periods across the 21<sup>st</sup> century, and  
181 find that these averages differ from the same quantity averaged over ten-year time slices by less  
182 than 20%, which is much less than the discrepancies caused by using different climate models in  
183 future predictions (Sheffield et al., 2013). This relatively small difference gives us confidence that



184 five-year simulations in GEOS-Chem will suffice for this study. We therefore perform two five-  
185 year time slice simulations for each RCP, covering the present day (2011-2015) and the late-21<sup>st</sup>  
186 century (2096-2100). The GEOS-Chem simulations are driven with present-day MERRA-2  
187 reanalysis meteorology from NASA/GMAO (Gelaro et al., 2017) to isolate the effect of changing  
188 wildfires on U.S. air quality. The simulations include emissions of all primary PM and the gas-  
189 phase precursors to secondary particles, with non-fire particle sources comprising fossil fuel  
190 combustion from transportation, industry, and power plants from the 2011 EPA NEI inventory. In  
191 the future time slices, non-fire emissions remain fixed at present-day levels.

192 Our study focuses on carbonaceous PM (smoke PM; BC+OC), which are the main  
193 components in wildfire smoke (Chow et al., 2011). For the present day, we apply 5-year (2011-  
194 2015) averaged GFED4s emissions to those regions that fall outside national forests and parks and  
195 temporally changing LPJ-LMfire emissions from the two RCPs within the Forests. Implementing  
196 the combined emissions allow us to further validate the simulated results in this study using  
197 observations from the Interagency Monitoring of Protected Visual Environments (IMPROVE)  
198 network (Figs. S5-S6). For the future time slices, we assume that fires outside national forests and  
199 parks remain at present-day levels, and we again combine the 2011-2015 GFED4s fire emissions  
200 with the temporally changing, future LPJ-LMfire emissions over the national forests and parks.

201

## 202 **3 Results**

### 203 **3.1 Spatial shifts in fire activity**

204 Under both RCPs, 21<sup>st</sup> century climate change and increasing atmospheric CO<sub>2</sub>  
205 concentrations lead to shifts in the distribution of total living biomass and dry matter burned. Fig.  
206 1 shows the changes in monthly mean temperature and precipitation averaged zonally over grid

207 cells at each 1° latitude of the West, relative to the present day, defined as ~2010. Peak temperature  
208 enhancements in JAS occur between 36°-42° N for ~2050 and ~2100 in both RCPs, with a  
209 maximum enhancement of 4 °C for RCP4.5 and 6 °C for RCP8.5 in 2100. Significant decreases  
210 in JAS precipitation occur between 33°-45° N under RCP4.5 and at latitudes north of 39° N under  
211 RCP8.5 for ~2100. The maximum decrease in monthly precipitation over the West is ~40 kg m<sup>-2</sup>  
212 (~60%) in JAS under both RCPs. These warmer and drier conditions favor fire activity under future  
213 climate.

214         Fires and smoke production are dependent on fuel load, and throughout the 21<sup>st</sup> century,  
215 total living biomass in the WUS is primarily concentrated in northern forests (Fig. 2). For RCP4.5,  
216 living biomass exhibits significant enhancements in U.S. national forests and parks at latitudes  
217 north of 43° N in the 2050 time slice and north of 45° N in the 2100 time slice. North of 46° N,  
218 the change in living biomass at 2100 (~0.4 kg C m<sup>-2</sup>) is double that at 2050 (~0.2 kg C m<sup>-2</sup>). At  
219 latitudes south of 40°N, living biomass in RCP4.5 is generally invariant over the 21<sup>st</sup> century. In  
220 RCP8.5, living biomass also increases significantly near the Canadian border – e.g., as much as  
221 ~0.2 kg C m<sup>-2</sup> for the 2050 time slice and ~0.4 kg C m<sup>-2</sup> for the 2100 time slice, relative to the  
222 present day. In contrast, at latitudes between 42°-47° N in RCP8.5, total living biomass decreases  
223 by as much as -0.6 kg C m<sup>-2</sup> for ~2100. For both RCPs, these mid-century and late-century changes  
224 in total living biomass are significant ( $p < 0.05$ ) across nearly all latitudes. In RCP4.5, the spatial  
225 shifts of total living biomass are relatively weak from 2050 to 2100, consistent with the moderate  
226 climate scenario with gradual reduction in greenhouse gas emissions after 2050. However, under  
227 the continued-emissions climate scenario RCP8.5, total living biomass in these forests first  
228 increases by 2050 and then decreases by ~10% by 2100, indicating a strongly disturbed vegetation  
229 system due to climate change. Despite this decrease, living biomass in this scenario is still

230 abundant in the West in 2100, especially over the northern forests (not shown), suggesting that  
231 future climate change will not limit fuel load for fire ignition or spread. Table 1 summarizes these  
232 results.

233 LPJ-LMfire simulates boreal needleleaf evergreen and boreal and temperate summergreen  
234 (broadleaf) trees as the dominant plant functional types (PFTs) in the national forests and parks of  
235 the WUS; these PFTs together account for ~90% of the total biomass in our study domain. Changes  
236 over the 21<sup>st</sup> century (Fig. 2) reflect the changes in the growth and distribution of these PFTs, with  
237 increases in living biomass in the north and decreases in the south in both RCP scenarios (Fig. S7).  
238 In the 2100 time slice, vegetation shifts further north than in the 2050 time slice. The reasons for  
239 this shift can be traced to the climate regimes favored by different vegetation types, with temperate  
240 and boreal trees showing moderate to strong inclination in their growth along the north-south  
241 temperature gradient (Aitken et al., 2008). For example, the temperate broadleaf summergreen  
242 PFT favors regions with moderate mean annual temperatures and distinct warm and cool seasons  
243 (Jarvis and Leverenz, 1983), while boreal needleleaf evergreen generally occurs in colder climate  
244 regimes (Aerts, 1995). With rising temperatures, the living biomass of temperate summergreen  
245 trees increases in most states in the WUS, with maximum enhancement of +1.0 kg C m<sup>-2</sup> in western  
246 Washington, northern Montana, and Idaho by 2100 in RCP8.5 relative to 2010. Decreases in this  
247 vegetation type for this scenario occur in the south, as much as -0.5 kg C m<sup>-2</sup> in New Mexico. In  
248 contrast, boreal trees increase in only a few regions in the far north, with a substantial contraction  
249 in their abundance over much of the West, as much as -4.0 kg C m<sup>-2</sup> for boreal needleleaf evergreen  
250 by 2100 in RCP8.5 over the northern forests.

251 Simulated area burned from lightning-ignited fires in the national forests and parks of the  
252 WUS increases by ~30% by ~2050, and by ~50% by ~2100 for both RCPs (not shown),

253 comparable to the predicted 78% increase in lightning-caused area burned in the U.S. under a  
254 doubled CO<sub>2</sub> climate by Price and Rind, 1994b, which did not account for vegetation changes due  
255 to climate change or changing CO<sub>2</sub>. That study, however, projected an increase in lightning flashes  
256 and did not consider changing land cover. The changes in area burned we calculate at 2050 are  
257 also within the range of previous studies using statistical methods for this region (e.g., 54% in  
258 Spracklen et al., 2009 and 10-50% in Yue et al., 2013). Fig. 2 further shows that dry matter burned,  
259 a function of both area burned and fuel load, increases relative to the present at most latitudes at  
260 both 2050 and 2100 and in both RCPs. Year-to-year variations in dry matter burned are greater  
261 than those in living biomass due to variations in the meteorological conditions driving fire  
262 occurrence. Previous studies have found that interannual variability in wildfire activity is strongly  
263 associated with regional surface temperature (Westerling et al., 2006; Yue et al., 2013). In our  
264 study, we show that total living biomass mostly decreases at latitudes ~45° N by ~2100 under  
265 RCP8.5, but the peak enhancements in dry matter burned also occur at these latitudes. This finding  
266 indicates that the modeled changes in fire activity are driven by changes in meteorological  
267 conditions that favor fire, as well as by shifts towards more pyrophilic landscapes such as open  
268 woodlands and savannas. As with biomass, lightning-caused fires also shift northward over the 21<sup>st</sup>  
269 century, especially in RCP8.5. In this scenario, dry matter burned increases by as much as 35 g m<sup>-2</sup>  
270 mon<sup>-1</sup> across 40°-48°N at ~2100 compared to the present day. By 2100, the fire-season total dry  
271 matter burned over the forests in the West increases by 24.58 Tg/JAS (111%) under RCP4.5 and  
272 by 50.00 Tg/JAS (161%) in RCP8.5 (Table 1).

273           The spatial distributions of changes in total living biomass and dry matter burned are shown  
274 in Fig. 3. Under RCP4.5, moderate decreases in total living biomass (by as much as -2.5 kg C m<sup>-2</sup>)  
275 and increases in dry matter burned by 2100 (up to ~70 g m<sup>-2</sup> mon<sup>-1</sup>) are concentrated in central

276 Idaho, Wyoming, and Colorado. Large declines in total living biomass and enhancements in dry  
277 matter burned occur in the forests of Idaho and Montana by 2100 under RCP8.5, with a hotspot of  
278  $-5.0 \text{ kg C m}^{-2}$  in biomass and  $+100 \text{ g m}^{-2} \text{ mon}^{-1}$  in dry matter burned in Yellowstone National Park.  
279 Similar trends in total living biomass and dry matter burned are also predicted for the Sierra  
280 Nevada (SN) region in California (Fig. S8), with the region defined as in Yue et al., 2014. Predicted  
281 changes in dry matter burned over the SN forests by 2050 are 17-44%, comparable to the calculated  
282 future increases of 30-50% by Yue et al., 2014. We find significant increases in dry matter burned  
283 of 81% by 2100 under RCP8.5 in the SN region. Our results suggest that even as future climate  
284 change diminishes vegetation biomass in some regions of the WUS, sufficient fuel still exists to  
285 allow increases in fire activity and dry matter burned.

### 286 **3.2 Smoke PM**

287 Given the large uncertainty in secondary aerosol formation within smoke plumes (Ortega  
288 et al., 2013), we assume that smoke PM mainly consists of primary BC and OC. We calculate  
289 emissions of fire-specific BC and OC by combining the estimates of the dry matter burned with  
290 emission factors from Akagi et al., 2011, which are dependent on land cover type. Application of  
291 these emissions to GEOS-Chem allows us to simulate the transport and distribution of smoke PM  
292 across the WUS.

293 With increasing lightning fire activity in most of the national forest and park areas of the  
294 WUS over the 21<sup>st</sup> century, smoke PM shows modest enhancement for RCP4.5, but more  
295 substantial increases for RCP8.5 (Fig. 4). Smoke PM enhancements in RCP4.5 occur primarily  
296 over the forests along the state boundaries of Idaho, Montana, and Wyoming, with large increases  
297 by as much as  $\sim 10 \mu\text{g m}^{-3}$  in Yellowstone National Park. Scattered increases in smoke PM in  
298 RCP4.5 are also predicted over the forests in northern Colorado, northern California, western

299 Oregon, and central Arizona. In RCP8.5, smoke PM enhancements are widespread over the  
300 northern states of the WUS by 2100, with significant increases in regions east of the Rocky  
301 Mountains. Increased fire activity and large smoke PM enhancements are seen by 2100 in RCP8.5,  
302 including large areas of the Flathead (Montana), Nez Perce-Clearwater (Idaho), and Arapaho and  
303 Roosevelt (Colorado) National Forests. Particularly large increases – as much as  $\sim 40 \mu\text{g m}^{-3}$  – occur  
304 in Yellowstone National Park (Wyoming). The increases in fire in these forests significantly  
305 influences air quality over the entire area of Idaho, Montana, Wyoming, and Colorado, with effects  
306 extending eastward to Nebraska and the Dakotas. Increased smoke PM is also predicted over the  
307 Sierra Nevada in both RCPs. In RCP4.5, average smoke PM over the entire WUS increases by 53%  
308 compared to present (Table 1). For RCP8.5, smoke PM more than doubles (109% increase) at  
309  $\sim 2100$ .

310

#### 311 **4 Discussion**

312 We apply an offline, coupled modeling approach to investigate the impact of changes in  
313 climate and vegetation on future lightning-caused wildfires and smoke pollution across the  
314 national forests and parks of the WUS in the 21<sup>st</sup> century. The GISS model predicts a warmer and  
315 drier climate but nearly constant lightning frequency in both scenarios. For RCP4.5, the late-21<sup>st</sup>  
316 century lightning-caused wildfire-specific smoke PM in the national forests and parks of the West  
317 increases  $\sim 53\%$  relative to present. Comparable fire activity between 2050 and 2100 reflect the  
318 effectiveness of the emission reduction strategies after 2050 under RCP4.5, as temperature changes  
319 across the West are relatively flat from 2050 to 2100, with a nearly constant area-averaged mean  
320 annual temperature of  $\sim 19.2^\circ\text{C}$ . In RCP8.5, mean annual temperatures continue increasing over  
321 the second half of the 21<sup>st</sup> century across the West, nearly  $2.1^\circ\text{C}$  from 2050, and wildfire-specific

322 PM concentrations double by 2100. Increased fire activity is driven by changes in meteorological  
323 conditions that favor fire, as well as by shifts towards more pyrophilic landscapes such as open  
324 woodlands and savannas.

325 In Table 2 we compare predictions in this study with previous fire estimates under future  
326 climate. A difference between these studies and ours is that we consider only changes in fire  
327 activity over the national forests and parks while others examine changes over the whole WUS.  
328 However, we find that in the GFED4s inventory, present-day fire emissions outside these federally  
329 managed areas contribute less than 1% of total DM in the WUS. For area burned, the fraction  
330 outside national forests and parks could be higher than 1%. In contrast, national forests and parks  
331 have abundant fuel supplies, making their fractional contribution to total DM much higher than  
332 would be implied by their fractional contribution to area burned. Also, the fact that lightning is the  
333 dominant driver of wildfire activity over the WUS forests (Balch et al., 2017) allows a reasonable  
334 comparison of the estimates in this study with those in previous studies that include both lightning  
335 and human-started fires over the West.

336 Table 2 shows that fire activity in the U.S. is predicted to increase in all studies cited. However,  
337 the projected changes in fire metrics such as area burned or in emissions or concentrations of  
338 smoke vary greatly across studies, from ~10-300% relative to present-day values. These  
339 discrepancies arise from differences in the methodologies, fire assumptions, future scenarios  
340 applied, domain and time period considered, and model resolution. The ~80% increases in smoke  
341 emissions that we project by 2050 is generally lower than estimates in previous statistical studies  
342 (e.g., 150-170% in Yue et al., 2013 or 100% in Spracklen et al., 2009). In contrast, the ~80%  
343 increase in smoke emissions in this study at ~2050 are substantially higher than the ~40% increases  
344 predicted by Ford et al., 2018 over the West, though the magnitudes of emission changes in the

345 two studies are similar. As in our study, Ford et al., 2018 relied on a land cover model, but they  
346 also attempted to account for the influence of future changes in meteorology and population on  
347 the suppression and ignition of fires. Ford et al., 2018 predicted scattered emission increases of  
348 40-45% over the West and a large increase of 85-220% over the Southeast due to increasing  
349 population and the role of human ignition. However, human activities have diverse impacts on  
350 wildfires, and those impacts are a function of land management policy, economics, and other social  
351 trends, making it challenging to predict how trends in human ignitions, fuel treatment, and fire  
352 suppression will evolve in the future (Fusco et al., 2016). In our study, we confine our focus to  
353 fires in national forests and parks in the West, where human activities such as landscape  
354 fragmentation through land use are less important. We further find that the patterns of increasing  
355 fire emissions by 2100 in our study – i.e., over the forests in northern Idaho, western Montana, and  
356 over the U.S. Pacific Northwest – are similar to those predicted by other studies, including Rogers  
357 et al., 2011 and Ford et al., 2018. Our study also predicts significantly elevated smoke PM in Utah,  
358 Wyoming, and Colorado in the late-21<sup>st</sup> century under RCP8.5 and in regions east of the Rocky  
359 Mountains because of the prevailing westerly winds.

360 The following limitations apply to our study. The vegetation model simulations of biomass  
361 and fire are driven by meteorology from just one climate model, GISS-E2-R. Over the WUS, this  
362 model simulates future temperature changes at the low end of projections by the CMIP5 ensemble,  
363 making our predictions of future fire conservative (Sheffield et al., 2013; Ahlström et al., 2012;  
364 Rupp et al., 2013). Also, the GEOS-Chem simulations are driven with present-day MERRA-2  
365 meteorology. Besides changes in fire emissions, future work could examine how changing  
366 meteorology may further influence smoke lifetime and transport processes, and investigate the  
367 feedback of fire on meteorology by developing an online coupled modeling approach.



368 Anthropogenic ignitions are not considered in this study, but fire behavior and therefore burned  
369 area simulated by LPJ-LMfire are primarily governed by meteorology and fuel structure. The fire  
370 simulations are performed on a  $0.5^{\circ} \times 0.5^{\circ}$  grid, which cannot capture some the fine-grain structure  
371 of the complex topography and sharp ecotones present in our study area (e.g., Shafer et al., 2015).  
372 Our study also does not consider the effects of future climate change on the transport or lifetime  
373 of smoke PM, nor the feedback of smoke aerosols on regional climate. Previous work, however,  
374 has shown that climate effects on smoke PM are likely to be small relative to the effect of changing  
375 wildfire activity (Spracklen et al., 2009).

376 Within these limitations, our results highlight the vulnerability of the WUS to lightning-  
377 caused wildfire in a changing climate. Even though a changing climate decreases the living  
378 biomass in some regions, we find that ample vegetation exists to fuel increases in fire activity and  
379 smoke. Especially strong enhancements in smoke PM occur in the Northern Rockies in the late-  
380 21<sup>st</sup> century under both the moderate and strong future emissions scenarios, suggesting that climate  
381 change will have a large, detrimental impact on air quality, visibility, and human health in a region  
382 valued for its national forests and parks. Our study thus provides a resource for environmental  
383 managers to better prepare for air quality challenges under a future climate change regime.

384

385

386

#### 387 **Data availability**

388 Data related to this paper may be requested from the authors.

389

#### 390 **Author contributions**

391 Y.L. conceived and designed the study, performed the GEOS-Chem simulations, analyzed the data,  
392 and wrote the manuscript, with contributions from all coauthors. J.O.K. performed the LPJ-LMfire  
393 simulations.

394

### 395 **Competing interests**

396 The authors declare that they have no competing interest.

397

### 398 **Acknowledgments**

399 This research was developed under Assistance Agreements 83587501 and 83587201 awarded by  
400 the U.S. Environmental Protection Agency (EPA). It has not been formally reviewed by the EPA.

401 The views expressed in this document are solely those of the authors and do not necessarily reflect  
402 those of the EPA. We thank all of the data providers of the datasets used in this study. PM data  
403 was provided by the Interagency Monitoring of Protected Visual Environments (IMPROVE;  
404 available online at <http://vista.cira.colostate.edu/improve>). IMPROVE is a collaborative  
405 association of state, tribal, and federal agencies, and international partners. U.S. Environmental  
406 Protection Agency is the primary funding source, with contracting and research support from the  
407 National Park Service. JOK is grateful for access to computing resources provided by the School  
408 of Geography and the Environment, University of Oxford. The Air Quality Group at the University  
409 of California, Davis is the central analytical laboratory, with ion analysis provided by the Research  
410 Triangle Institute, and carbon analysis provided by the Desert Research Institute. We acknowledge  
411 the World Climate Research Programme's Working Group on Coupled Modelling, which is  
412 responsible for CMIP, and we thank the group of NASA Goddard Institute for Space Studies for  
413 producing and making available their GISS-E2-R climate model output. For CMIP the U.S.

414 Department of Energy's Program for Climate Model Diagnosis and Intercomparison provides  
415 coordinating support and led development of software infrastructure in partnership with the Global  
416 Organization for Earth System Science Portals. The GISS-E2-R dataset were downloaded from  
417 <https://cmip.llnl.gov/cmip5/>. We thank the Land-use Harmonization team for producing the  
418 harmonized set of land-use scenarios and making available the dataset online at  
419 <http://tntcat.iiasa.ac.at/RcpDb/>. We also thank X. Yue for providing the raster of southern  
420 California.

421 **References**

- 422 Abatzoglou, J. T., Kolden, C. A., Balch, J. K., and Bradley, B. A.: Controls on interannual  
423 variability in lightning-caused fire activity in the western US, *Environmental Research*  
424 *Letters*, 11, 045005, 2016.
- 425 Abatzoglou, J. T., and Williams, A. P.: Impact of anthropogenic climate change on wildfire  
426 across western US forests, *Proceedings of the National Academy of Sciences*, 113, 11770-  
427 11775, 2016.
- 428 Aerts, R.: The advantages of being evergreen, *Trends in ecology & evolution*, 10, 402-407, 1995.
- 429 Ahlström, A., Schurgers, G., Arneth, A., and Smith, B.: Robustness and uncertainty in terrestrial  
430 ecosystem carbon response to CMIP5 climate change projections, *Environmental Research*  
431 *Letters*, 7, 044008, 2012.
- 432 Aitken, S. N., Yeaman, S., Holliday, J. A., Wang, T., and Curtis-McLane, S.: Adaptation,  
433 migration or extirpation: climate change outcomes for tree populations, *Evolutionary*  
434 *applications*, 1, 95-111, 2008.
- 435 Akagi, S., Yokelson, R. J., Wiedinmyer, C., Alvarado, M., Reid, J., Karl, T., Crouse, J., and  
436 Wennberg, P.: Emission factors for open and domestic biomass burning for use in  
437 atmospheric models, *Atmospheric Chemistry and Physics*, 11, 4039-4072, 2011.
- 438 Altaratz, O., Kucienska, B., Kostinski, A., Raga, G. B., and Koren, I.: Global association of  
439 aerosol with flash density of intense lightning, *Environmental Research Letters*, 12, 114037,  
440 2017.
- 441 Archibald, S., Roy, D. P., van Wilgen, B. W., and Scholes, R. J.: What limits fire? An  
442 examination of drivers of burnt area in Southern Africa, *Global Change Biology*, 15, 613-630,  
443 2009.
- 444 Balch, J. K., Bradley, B. A., Abatzoglou, J. T., Nagy, R. C., Fusco, E. J., and Mahood, A. L.:  
445 Human-started wildfires expand the fire niche across the United States, *Proceedings of the*  
446 *National Academy of Sciences*, 114, 2946-2951, 2017.
- 447 Brey, S. J., Barnes, E. A., Pierce, J. R., Wiedinmyer, C., and Fischer, E. V.: Environmental  
448 conditions, ignition type, and air quality impacts of wildfires in the southeastern and western  
449 United States, *Earth's future*, 6, 1442-1456, 2018.
- 450 Brovkin, V., Boysen, L., Arora, V., Boisier, J., Cadule, P., Chini, L., Claussen, M.,  
451 Friedlingstein, P., Gayler, V., and Van Den Hurk, B.: Effect of anthropogenic land-use and  
452 land-cover changes on climate and land carbon storage in CMIP5 projections for the twenty-  
453 first century, *Journal of Climate*, 26, 6859-6881, 2013.
- 454 Chaste, E., Girardin, M. P., Kaplan, J. O., Portier, J., Bergeron, Y., and Hély, C.: The  
455 pyrogeography of eastern boreal Canada from 1901 to 2012 simulated with the LPJ-LMfire  
456 model, *Biogeosciences*, 15, 1273-1292, 10.5194/bg-15-1273-2018, 2018.
- 457 Chow, J. C., Watson, J. G., Lowenthal, D. H., Chen, L.-W. A., and Motallebi, N.: PM2.5 source  
458 profiles for black and organic carbon emission inventories, *Atmospheric Environment*, 45,  
459 5407-5414, 2011.
- 460 Flannigan, M. D., Stocks, B. J., and Wotton, B. M.: Climate change and forest fires, *Science of*  
461 *the total environment*, 262, 221-229, 2000.
- 462 Ford, B., Val Martin, M., Zelasky, S., Fischer, E., Anenberg, S., Heald, C., and Pierce, J.: Future  
463 fire impacts on smoke concentrations, visibility, and health in the contiguous United States,  
464 *GeoHealth*, 2, 229-247, 2018.

465 Fusco, E. J., Abatzoglou, J. T., Balch, J. K., Finn, J. T., and Bradley, B. A.: Quantifying the  
466 human influence on fire ignition across the western USA, *Ecological applications*, 26, 2390-  
467 2401, 2016.

468 Gelaro, R., McCarty, W., Suárez, M. J., Todling, R., Molod, A., Takacs, L., Randles, C. A.,  
469 Darnenov, A., Bosilovich, M. G., and Reichle, R.: The modern-era retrospective analysis for  
470 research and applications, version 2 (MERRA-2), *Journal of Climate*, 30, 5419-5454, 2017.

471 Giglio, L., Randerson, J. T., and van der Werf, G. R.: Analysis of daily, monthly, and annual  
472 burned area using the fourth-generation global fire emissions database (GFED4), *Journal of*  
473 *Geophysical Research: Biogeosciences*, 118, 317-328, 2013.

474 Hamilton, D. S., Hantson, S., Scott, C., Kaplan, J., Pringle, K., Nieradzik, L., Rap, A., Folberth,  
475 G., Spracklen, D., and Carslaw, K.: Reassessment of pre-industrial fire emissions strongly  
476 affects anthropogenic aerosol forcing, *Nature communications*, 9, 3182, 2018.

477 Jarvis, P., and Leverenz, J.: Productivity of temperate, deciduous and evergreen forests, in:  
478 *Physiological plant ecology IV*, Springer, 233-280, 1983.

479 Kumar, S., Dirmeyer, P. A., Merwade, V., DelSole, T., Adams, J. M., and Niyogi, D.: Land  
480 use/cover change impacts in CMIP5 climate simulations: A new methodology and 21st  
481 century challenges, *Journal of Geophysical Research: Atmospheres*, 118, 6337-6353, 2013.

482 Li, F., Val Martin, M., Andreae, M. O., Arneth, A., Hantson, S., Kaiser, J. W., Lasslop, G., Yue,  
483 C., Bachelet, D., and Forrest, M.: Historical (1700–2012) global multi-model estimates of the  
484 fire emissions from the Fire Modeling Intercomparison Project (FireMIP), 2019.

485 Liu, J. C., Wilson, A., Mickley, L. J., Dominici, F., Ebisu, K., Wang, Y., Sulprizio, M. P., Peng,  
486 R. D., Yue, X., and Son, J.-Y.: Wildfire-specific Fine Particulate Matter and Risk of Hospital  
487 Admissions in Urban and Rural Counties, *Epidemiology (Cambridge, Mass.)*, 28, 77-85,  
488 2017.

489 Magi, B. I.: Global Lightning Parameterization from CMIP5 Climate Model Output, *Journal of*  
490 *Atmospheric and Oceanic Technology*, 32, 434-452, 10.1175/jtech-d-13-00261.1, 2015.

491 Nadelhoffer, K. J., Emmett, B. A., Gundersen, P., Kjønaas, O. J., Koopmans, C. J., Schleppi, P.,  
492 Tietema, A., and Wright, R. F.: Nitrogen deposition makes a minor contribution to carbon  
493 sequestration in temperate forests, *Nature*, 398, 145, 1999.

494 Nazarenko, L., Schmidt, G., Miller, R., Tausnev, N., Kelley, M., Ruedy, R., Russell, G., Aleinov,  
495 I., Bauer, M., and Bauer, S.: Future climate change under RCP emission scenarios with GISS  
496 ModelE2, *Journal of Advances in Modeling Earth Systems*, 7, 244-267, 2015.

497 Ortega, A., Day, D., Cubison, M., Brune, W., Bon, D., De Gouw, J., and Jimenez, J.: Secondary  
498 organic aerosol formation and primary organic aerosol oxidation from biomass-burning  
499 smoke in a flow reactor during FLAME-3, *Atmospheric Chemistry and Physics*, 13, 11551-  
500 11571, 2013.

501 Park, R. J., Jacob, D. J., Chin, M., and Martin, R. V.: Sources of carbonaceous aerosols over the  
502 United States and implications for natural visibility, *Journal of Geophysical Research:*  
503 *Atmospheres*, 108, 2003.

504 Park, R. J., Jacob, D. J., Field, B. D., Yantosca, R. M., and Chin, M.: Natural and transboundary  
505 pollution influences on sulfate-nitrate-ammonium aerosols in the United States: Implications  
506 for policy, *Journal of Geophysical Research: Atmospheres*, 109, 2004.

507 Pechony, O., and Shindell, D. T.: Driving forces of global wildfires over the past millennium and  
508 the forthcoming century, *Proceedings of the National Academy of Sciences*, 107, 19167-  
509 19170, 2010.

510 Pfeiffer, M., Spessa, A., and Kaplan, J. O.: A model for global biomass burning in preindustrial  
511 time: LPJ-LMfire (v1. 0), *Geoscientific Model Development*, 6, 643-685, 2013.

512 Pierce, J., Val Martin, M., and Heald, C.: Estimating the effects of changing climate on fires and  
513 consequences for US air quality, using a set of global and regional climate models—Final  
514 report to the Joint Fire Science Program, Fort Collins (CO): Joint Fire Science Program, 2017.

515 Price, C., and Rind, D.: Possible implications of global climate change on global lightning  
516 distributions and frequencies, *Journal of Geophysical Research: Atmospheres*, 99, 10823-  
517 10831, 1994a.

518 Price, C., and Rind, D.: The impact of a 2× CO<sub>2</sub> climate on lightning-caused fires, *Journal of*  
519 *Climate*, 7, 1484-1494, 1994b.

520 Rogers, B. M., Neilson, R. P., Drapek, R., Lenihan, J. M., Wells, J. R., Bachelet, D., and Law, B.  
521 E.: Impacts of climate change on fire regimes and carbon stocks of the US Pacific Northwest,  
522 *Journal of Geophysical Research: Biogeosciences*, 116, 2011.

523 Romps, D. M., Seeley, J. T., Vollaro, D., and Molinari, J.: Projected increase in lightning strikes  
524 in the United States due to global warming, *Science*, 346, 851-854, 2014.

525 Rupp, D. E., Abatzoglou, J. T., Hegewisch, K. C., and Mote, P. W.: Evaluation of CMIP5 20th  
526 century climate simulations for the Pacific Northwest USA, *Journal of Geophysical Research:*  
527 *Atmospheres*, 118, 10,884-810,906, 2013.

528 Shafer, S. L., Bartlein, P. J., Gray, E. M., and Peltier, R. T.: Projected Future Vegetation  
529 Changes for the Northwest United States and Southwest Canada at a Fine Spatial Resolution  
530 Using a Dynamic Global Vegetation Model, *PLoS One*, 10, e0138759,  
531 10.1371/journal.pone.0138759, 2015.

532 Sheffield, J., Barrett, A. P., Colle, B., Nelun Fernando, D., Fu, R., Geil, K. L., Hu, Q., Kinter, J.,  
533 Kumar, S., and Langenbrunner, B.: North American climate in CMIP5 experiments. Part I:  
534 Evaluation of historical simulations of continental and regional climatology, *Journal of*  
535 *Climate*, 26, 9209-9245, 2013.

536 Sitch, S., Smith, B., Prentice, I. C., Arneeth, A., Bondeau, A., Cramer, W., Kaplan, J. O., Levis,  
537 S., Lucht, W., Sykes, M. T., Thonicke, K., and Venevsky, S.: Evaluation of ecosystem  
538 dynamics, plant geography and terrestrial carbon cycling in the LPJ dynamic global  
539 vegetation model, *Global Change Biology*, 9, 161-185, 10.1046/j.1365-2486.2003.00569.x,  
540 2003.

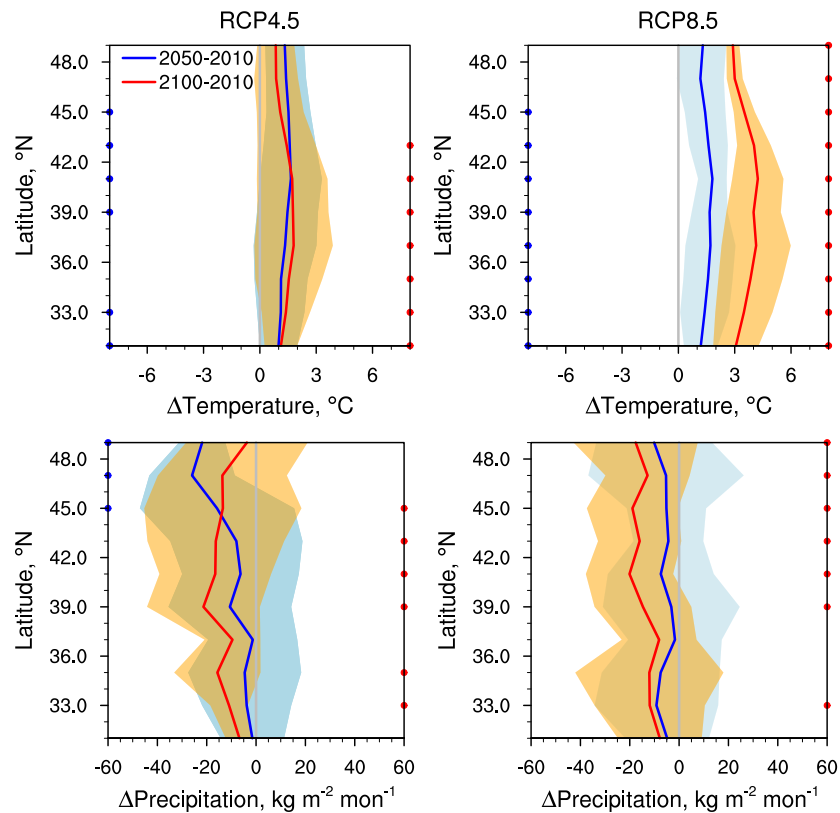
541 Spracklen, D. V., Mickley, L. J., Logan, J. A., Hudman, R. C., Yevich, R., Flannigan, M. D., and  
542 Westerling, A. L.: Impacts of climate change from 2000 to 2050 on wildfire activity and  
543 carbonaceous aerosol concentrations in the western United States, *Journal of Geophysical*  
544 *Research: Atmospheres*, 114, 2009.

545 Val Martin, M., Honrath, R., Owen, R. C., Pfister, G., Fialho, P., and Barata, F.: Significant  
546 enhancements of nitrogen oxides, black carbon, and ozone in the North Atlantic lower free  
547 troposphere resulting from North American boreal wildfires, *Journal of Geophysical*  
548 *Research: Atmospheres*, 111, 2006.

549 Val Martin, M., Heald, C., Lamarque, J.-F., Tilmes, S., Emmons, L., and Schichtel, B.: How  
550 emissions, climate, and land use change will impact mid-century air quality over the United  
551 States: a focus on effects at national parks, *Atmospheric Chemistry and Physics*, 15, 2805-  
552 2823, 2015.

553 Westerling, A., and Bryant, B.: Climate change and wildfire in California, *Climatic Change*, 87,  
554 231-249, 2008.

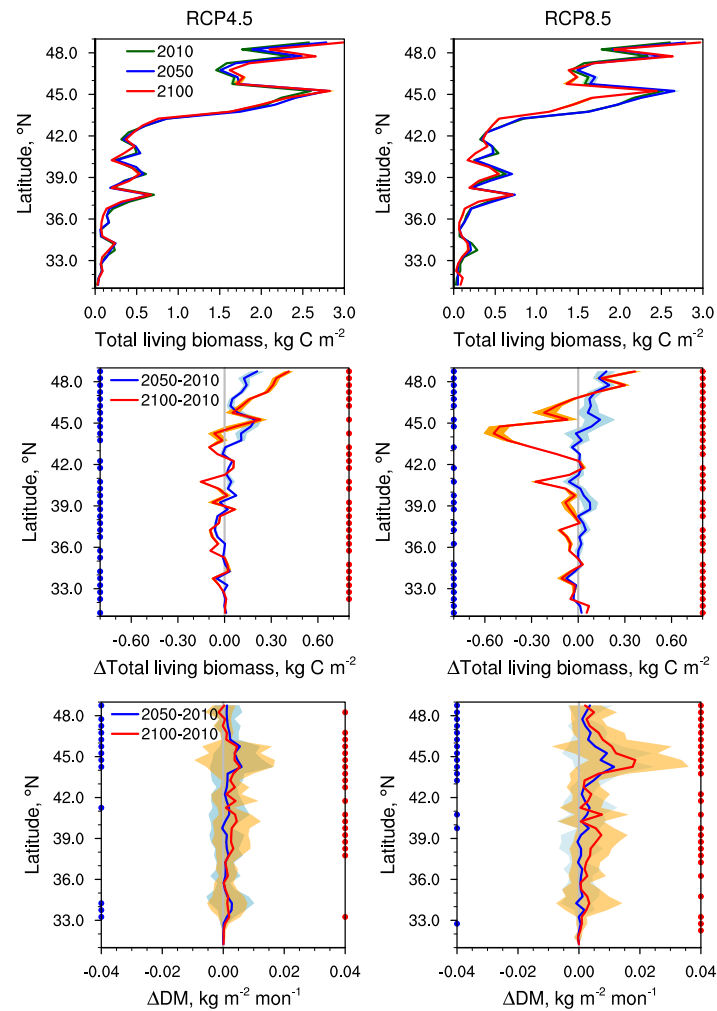
555 Westerling, A. L., Hidalgo, H. G., Cayan, D. R., and Swetnam, T. W.: Warming and earlier  
556 spring increase western US forest wildfire activity, *science*, 313, 940-943, 2006.  
557 Westerling, A. L.: Increasing western US forest wildfire activity: sensitivity to changes in the  
558 timing of spring, *Philosophical Transactions of the Royal Society B: Biological Sciences*, 371,  
559 20150178, 2016.  
560 Wotton, B., Martell, D., and Logan, K.: Climate change and people-caused forest fire occurrence  
561 in Ontario, *Climatic Change*, 60, 275-295, 2003.  
562 Yue, X., Mickley, L. J., Logan, J. A., and Kaplan, J. O.: Ensemble projections of wildfire activity  
563 and carbonaceous aerosol concentrations over the western United States in the mid-21st  
564 century, *Atmospheric Environment*, 77, 767-780, 2013.  
565 Yue, X., Mickley, L. J., and Logan, J. A.: Projection of wildfire activity in southern California in  
566 the mid-twenty-first century, *Climate dynamics*, 43, 1973-1991, 2014.  
567



569

570 **Figure 1.** Modeled changes in temperature (top) and precipitation (bottom) in July-August-  
 571 September (JAS) at  $\sim$ 2050 and  $\sim$ 2100 as a function of latitude over the WUS for RCP4.5 (left)  
 572 and RCP8.5 (Nadelhoffer et al.). Changes are zonally averaged and relative to the present day  
 573 ( $\sim$ 2010), with 5-year averages in each time slice. The bold blue lines show the changes between  
 574 2010 and 2050, averaged over all longitudes in the WUS ( $31^{\circ}\text{N} - 49^{\circ}\text{N}$ ,  $100^{\circ}\text{W} - 125^{\circ}\text{W}$ ); bold  
 575 red lines show the mean changes between 2010 and 2100. Light blue and orange shadings  
 576 represent the temporal standard deviation across the 15 months (5 years  $\times$  3 months) of each time  
 577 slice. Blue dots along the axes mark those latitudes showing statistically significant differences  
 578 between the JAS 2010 and 2050 time slices ( $p < 0.05$ ); red dots mark those latitudes with  
 579 statistically significant differences at 2100. Temperatures and precipitations are from the GISS-  
 580 E2-R climate model.

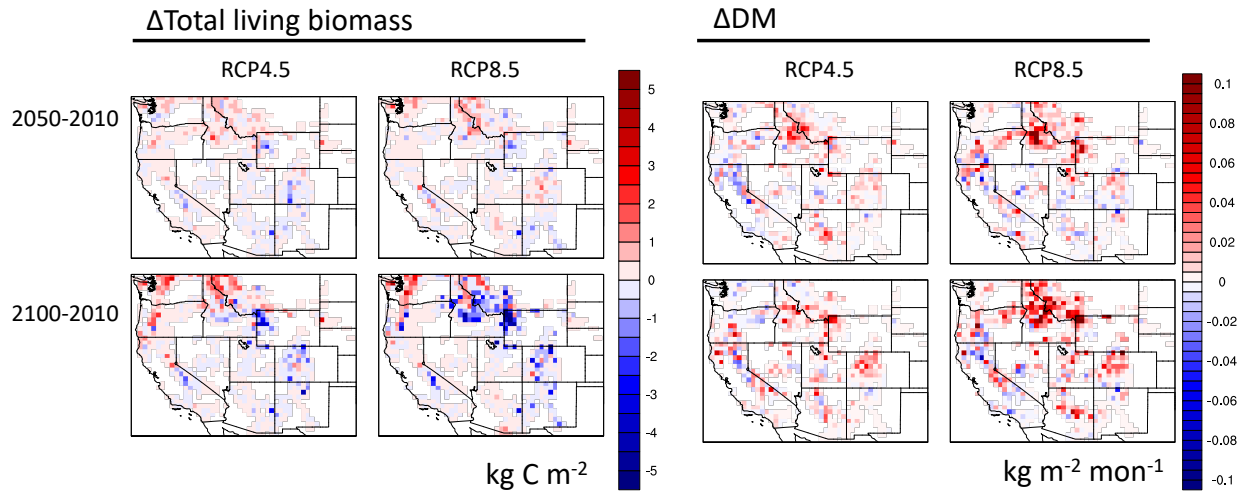




582

583 **Figure 2.** The top panel shows total living biomass at ~2010, ~2050 and ~2100 as a function of  
 584 latitude over the WUS for RCP4.5 (left) and RCP8.5 (Nadelhoffer et al.), with 5-year averages in  
 585 each time slice. The lower four panels are as in Figure 1, but for changes in total living biomass  
 586 (middle) and lightning-caused dry matter burned (DM; bottom) as a function of latitude over the  
 587 WUS. Results of living biomass and DM are from LPJ-LMfire. As in Figure 1, dots along the axes  
 588 mark those latitudes showing statistically significant differences.

589

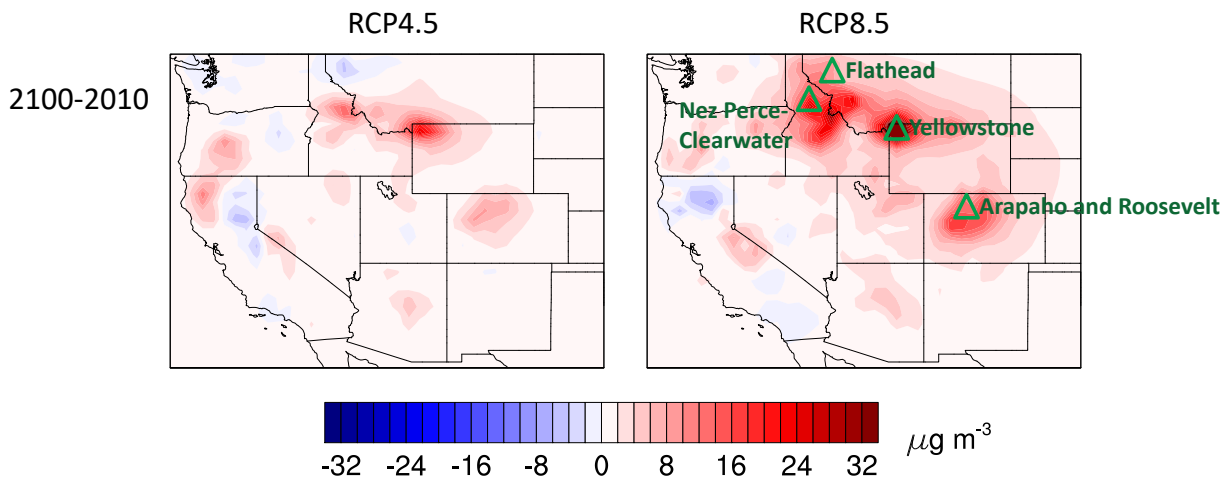


590

591 **Figure 3.** Simulated changes in yearly mean total living biomass and monthly mean DM averaged  
 592 over the fire season in the national forests and parks across the WUS for the RCP4.5 and RCP8.5  
 593 scenarios. The top row shows changes between the present day and 2050, and the bottom row  
 594 shows changes between the present day and 2100. Results are from LPJ-LMfire, with five years  
 595 representing each time period. The fire season is July, August, and September. White spaces  
 596 indicate areas outside the national forests and parks.

597

598



599

600 **Figure 4.** Simulated changes in fire-season smoke PM (BC+OC) at ~2100 relative to the present  
601 day for RCP4.5 and RCP8.5. Results are from GEOS-Chem at a spatial resolution  $0.5^\circ \times 0.625^\circ$ ,  
602 averaged over July, August, and September. Each time period is represented by a 5-year time slice.  
603 National parks and forests that experience large smoke PM enhancements are labeled by green  
604 triangles.

605

**Table 1.** Total living biomass, dry matter burned (DM), and smoke PM (BC+OC) emissions over national forests and parks in the WUS and smoke PM concentrations averaged across the entire West. Values for the present day (~2010) are shown in the top row; changes in ~2050 and ~2100 relative to the present day are shown in bottom two rows. Statistically significant changes are in boldface.

Time slices	Living biomass <sup>b</sup> , Tg/yr	DM <sup>b</sup> , Tg/JAS	BC+OC emission <sup>b</sup> , Tg/JAS	BC+OC <sup>c</sup> , $\mu\text{g m}^{-3}$				
	RCP4.5	RCP8.5	RCP4.5	RCP8.5	RCP4.5	RCP8.5		
2010 <sup>a</sup>	3074.8±33.7	3036.9±55.5	22.16±4.16	30.96±7.15	0.15±0.04	0.21±0.06	2.11±0.48	2.55±0.81
2050-2010 <sup>a</sup>	138.2±46.0	126.2±80.2	<b>18.0±16.1</b>	<b>26.7±14.8</b>	<b>0.15±0.13</b>	<b>0.23±0.15</b>	--	--
2100-2010 <sup>a</sup>	119.6±34.4	-270.7±76.1	<b>24.6±13.2</b>	<b>50.0±18.0</b>	<b>0.18±0.14</b>	<b>0.39±0.17</b>	<b>1.11±1.02</b>	<b>2.78±1.73</b>

<sup>a</sup> Each time slice represents 5 years; <sup>b</sup> Values are fire-season summations over national forests and parks;

<sup>c</sup> BC+OC concentrations are fire-season averages over the West; Statistical significance is not calculated for living biomass.

607 **Table 2.** Comparison of fire predictions in the U.S. under future climate.

<b>Methods</b>	<b>Region, scenarios, and future time slice</b>	<b>Fire metric and percent increase relative to present day</b>	<b>Smoke PM and percent increase relative to present day</b>	<b>Reference</b>
Statistical models for lightning fires	Entire U.S. Doubled CO <sub>2</sub> climate	Number of fires: 44% Area burned: 78%		Price and Rind, 1994b
Two climate models	Entire U.S. Doubled CO <sub>2</sub> climate ~2060	Seasonal fire severity rating: 10-50%		Flannigan et al., 2000
Statistical model	California, U.S. A2 ~2100	Large fire risk: 12-53%		Westerling and Bryant, 2008
Statistical models and GEOS-Chem	Western U.S. A1B ~2050	Area burned: 54% Smoke emission: 100%	Smoke PM concentrations BC: 20% OC: 40%	Spracklen et al., 2009
Climate model with global-scale fire parameterization	Global B1, A1B, A2 ~2100	Fire occurrence in the western U.S. B1: 120% A1B: 233% A2: 242%		Pechony and Shindell, 2010
MAPSS-CENTURY 1 dynamic general vegetation model	U.S. Pacific Northwest A2 ~2100	Area burned: 76-310% Burn severity: 29-41%		Rogers et al., 2011
Statistical models + GEOS-Chem	Western U.S. A1B ~2050	Area burned: 63-169% Smoke PM emissions: 150-170%	Smoke PM concentrations: 43-55%	Yue et al., 2013
Statistical models	California, U.S. A1B ~2050	Area burned: 10-100%		Yue et al., 2014
Coupled Community Land Model (CLMv4) and Community Earth System Model (CESM) <sup>2</sup>	Western U.S. RCP4.5 and RCP8.5 ~2050	Smoke PM emissions: • RCP4.5: 100% • RCP8.5: 50%	Total PM <sub>2.5</sub> concentrations <sup>1</sup> • RCP4.5: 22% • RCP8.5: 63%	Val Martin et al., 2015

CLMv4.5-BGC with fire parameterization coupled with CESM <sup>3</sup>	Contiguous U.S. RCP4.5 and RCP8.5 ~2050 and ~2100  Relative to the present day (1995-2005)	Area burned by 2050: • RCP4.5: 67% • RCP8.5: 50% by 2100: • RCP4.5: 58% • RCP8.5: 108%	Total PM <sub>2.5</sub> concentrations <sup>1</sup> by 2050: • RCP4.5: 146% • RCP8.5: 85% by 2100: • RCP4.5: 108% • RCP8.5: 246%	Pierce et al., 2017
CLMv4.5 with fire parameterization coupled with CESM <sup>3</sup>	Contiguous U.S. RCP4.5 & RCP8.5 ~2050 and ~2100  Relative to the present day (2000-2010)	Smoke PM emissions by 2050: • RCP4.5: 126% • RCP8.5: 54% by 2100: • RCP4.5: 125% • RCP8.5: 149%  by 2050 over the West: • RCP4.5: 45% • RCP8.5: 40%	Total PM <sub>2.5</sub> concentrations <sup>1</sup> by 2050: • RCP4.5: 113% • RCP8.5: 27% by 2100: • RCP4.5: 93% • RCP8.5: 127%	Ford et al., 2018
LPJ-LMfire coupled with GEOS-Chem	Western U.S. RCP4.5 and RCP8.5 ~2050 and ~2100  Relative to the present day (2011-2015)	Smoke PM emissions by 2050: • RCP4.5: 81% • RCP8.5: 86% by 2100: • RCP4.5: 111% • RCP8.5: 161%	Smoke PM concentrations by 2100: • RCP4.5: 53% • RCP8.5: 109%	This study

608 <sup>1</sup> Total PM<sub>2.5</sub> is the combination of sulfate, ammonium nitrate, secondary organic aerosols, fine  
609 dust, fine sea salt, BC and OC.

610 <sup>2</sup> This model considers changes in climate, anthropogenic emissions, land cover, and land use.

611 <sup>3</sup> This model considers changes in climate, anthropogenic emissions, land cover, land use, and  
612 population.  
613